Statistical Methods for Detecting Stellar Occultations by Kuiper Belt Objects: the Taiwanese-American Occultation Survey

Chyng-Lan Liang[*] John A. Rice[†] Imke de Pater[‡] Charles Alcock[§]
Tim Axelrod[¶] Andrew Wang[‖] Stuart Marshall[**]

September 3, 2002

Abstract

The Taiwanese-American Occultation Survey (TAOS) will detect objects in the Kuiper Belt, by measuring the rate of occultations of stars by these objects, using an array of three to four 50cm wide-field robotic telescopes. Thousands of stars will be monitored, resulting in hundreds of millions of photometric measurements per night. To optimize the success of TAOS, we have investigated various methods of gathering and processing the data and developed statistical methods for detecting occultations. In this paper we discuss these methods. The resulting estimated detection efficiencies will be used to guide the choice of various operational parameters determining the mode of actual observation when the telescopes come on line and begin routine observations. In particular we show how real-time detection algorithms may be constructed, taking advantage of having multiple telescopes. We also discuss a retrospective method for estimating the rate at which occultations occur.

1   Introduction

Since the middle of the last century, there has been increasing speculation that a residual proto-planetary disk existed beyond Neptune consisting of a vast number of remnants of the accretional phase of the early evolution of the solar system. This belt is the source of most short–period comets, those with periods of 200 years or less [Edgeworth, 1949], [Kuiper, 1951], [Fernandez, 1980]. Observational success was first achieved with the discovery of 1992QB1 [Jewitt and Luu, 1993]. Major observational efforts since then have identified about 500 objects, the largest having a diameter of about 900km. Studies of the Kuiper belt have been reviewed in [Weissman, 1995], [Stern, 1996] and [Jewitt, 1999].

At 50AU (one AU is the average distance from the Sun to Earth, 1.49×10^8 km,), we can currently only directly observe objects larger than around 100km, since smaller objects do not reflect sufficient light. Thus, other methods are needed to detect smaller objects, which are far

---

[*]Department of Statistics, University of California, Berkeley. USA
[†]Department of Statistics, University of California, Berkeley. USA
[‡]Department of Astronomy, University of California, Berkeley. USA
[§]Department of Physics and Astronomy, University of Pennsylvania. USA
[¶]Steward Observatory, University of Arizona. USA
[‖]Academia Sinica, Institute of Astronomy and Astrophysics. Taiwan
[**]Institute of Geophysics and Planetary Physics, Lawrence Livermore National Laboratory. USA

greater in abundance. The idea of the occultation technique [Bailey, 1976], [Axelrod et al., 1992] is simply the following: One monitors the light from a sample of stars that have angular sizes smaller than the expected angular sizes of Kuiper Belt Objects (KBO's) we hope to detect. An occultation is manifested by detecting the partial or total reduction in the flux from one of the stars for a brief interval, when a KBO passes between it and the observer. This technique will allow the detection of objects with a radius of only a few kilometers and/or larger objects lying beyond 100AU, objects which have thus far been undetectable by direct observation.

The Taiwanese-American Occultation Survey (TAOS), a collaboration involving the Lawrence Livermore National Laboratory (USA), Academia Sinica and National Central University (both of Taiwan), will use this stellar occultation technique with an array of three or four wide-field robotic telescopes to estimate the number of KBOs of size greater than a few kilometers. Each of these 50cm telescopes will be pointed at the same 3 square degrees of the sky and will record light from the same approximately 2,000 stars. The telescope array will be located in the Yu Shan (Jade Mountain) area of central Taiwan (longitude $120°$ 50' 28" E; latitude $23°$ 30' N).

The detection scheme will need to operate in real-time, as the data is being gathered, in order to alert more powerful telescopes for followup. It is anticipated that a large amount of data will be generated on a nightly basis, yielding about 10,000 gigabytes of data and $10^{10} - 10^{12}$ occultation tests per year. The challenge is to detect among these only small number of occultations, perhaps tens or hundreds (the uncertainty in this number reflects our ignorance).

2   TAOS Observing Scheme

The imaging system at each telescope will consist of a thermo-electrically cooled charge coupled device (CCD) camera with a 2048×2048 pixel CCD detector (pixel size is 2.89 arcseconds).

At the time the research presented here was conducted, the final selection of star fields had not yet been made, other than that they will be near the ecliptic plane (the plane of the Earth's orbit). Although naively one might think that the denser star fields might be more profitable for revealing occultations, the detection scheme has to deal with crowding of stars and sky background. We will thus consider both crowded and sparse fields (Figure 1).

The angle of observation will affect the properties of the occultation, since the relative velocity of the KBO with respect to Earth will depend upon it. The KBO is said to be observed at *quadrature* when the relative velocity is zero. The angle of quadrature depends upon the KBO's heliocentric distance (the distance to the center of the Sun). For a KBO at 50AU, the angle of observation at quadrature is around 80 degrees. The KBO is said to be observed at *opposition* when the relative velocity is at its maximum—for a KBO moving at 4km s^{-1} (which is typical for an object at 50AU), this maximal relative velocity is 26km s^{-1}, since Earth moves at about 30km s^{-1}. Figure 2 shows the KBO at opposition and at quadrature. The relative velocity of an object in a circular orbit at r AU, at angle of observation φ, is given by:

$$RV(r, \varphi) = v_e \cos \varphi - v_e \sqrt{\left(\frac{r_e}{r}\right)\left(1 - \left(\frac{r_e}{r}\right)^2 \sin^2 \varphi\right)} \tag{1}$$

where v_e and r_e are the velocity and heliocentric distance of the Earth respectively. We will consider two relative velocities: 20km s^{-1} (near opposition) and 6km s^{-1} (near quadrature).

The proposed mode of observation for TAOS is the following: we track the stars at the sidereal rate (the rate at which distant stars appear to move across the sky) for dt seconds, so that a star will always illuminate the same pixels, then rapidly shift the CCD counts with respect to the star
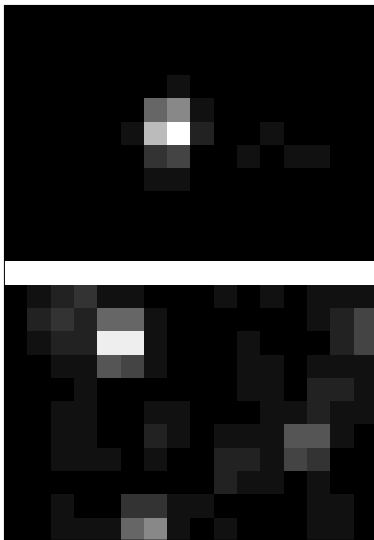
Figure 1: Two 46×32 arcsec. sections of simulated images for star fields (RA 4.905', Dec 29.275") [Top] and (RA 9.61833', Dec 0.7250") [Bottom].
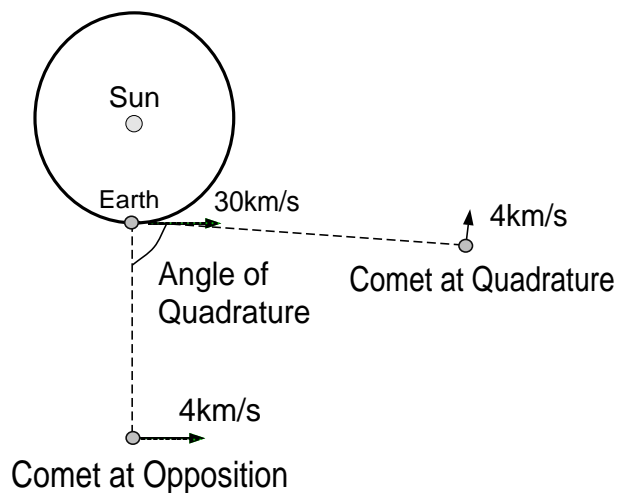

Figure 2: KBO at opposition and at quadrature.

by a set number of pixels, at set intervals of time. The "star trail" would then resemble a zipper, with clusters of counts at spaced intervals, which we refer to as *holds*, with the *holdtime dt*. Charge from successive rows of pixels will fall into the horizontal register of the CCD and may be read off. The resulting "exposures" are very long: data will be read out continuously and we will only close the shutters when we wish to monitor another star field. Figure 3 shows the data-taking process at two different time-points. Figure 4 shows a section of a simulated zipper mode image. The alternative to zipper mode would be to hold the telescope's position fixed so that the stars would produce trails across the CCD. A disadvantage to this latter scheme is that the shutter would have to be frequently closed and opened in order that the accumulated photons from the sky background did not overwhelm the trails, with consequent frequent shutter failures. It also turns out that detectability is higher in zipper mode.

Smearing resulting from the transit time between holds cannot be ignored. The pixels accumulate counts from the star as we wait for each row to be read off the horizontal register of the CCD. For a transit time of 1.3ms versus a holdtime of 200ms, the counts in the "transit" pixels will roughly be $1/150^{th}$ of the counts for the "hold" pixels. This may be a problem if we have a very bright star, which smears over a less bright star, even if the hold pixels do not coincide.

The degree of overlapping stars depends on the star field being monitored: typically the more crowded the field, the more overlapping occurs. The amount of overlapping, for any particular mode of observation, may be determined before observation begins. We note that, for shutterless zipper mode, with regularly spaced holds, except for the first few and last few observations, an overlapped hold will always be overlapped and an nonoverlapped hold will always be nonoverlapped.
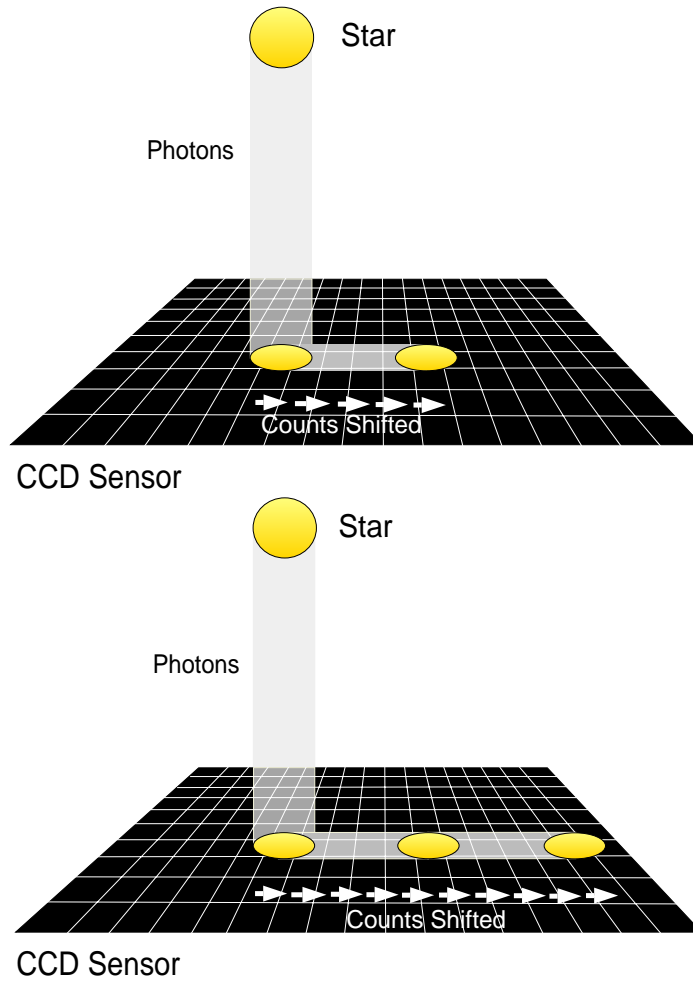
Figure 3: Zipper mode, with number of pixels between holds, $z = 5$. The figure at the top shows an earlier time than the one at the bottom.
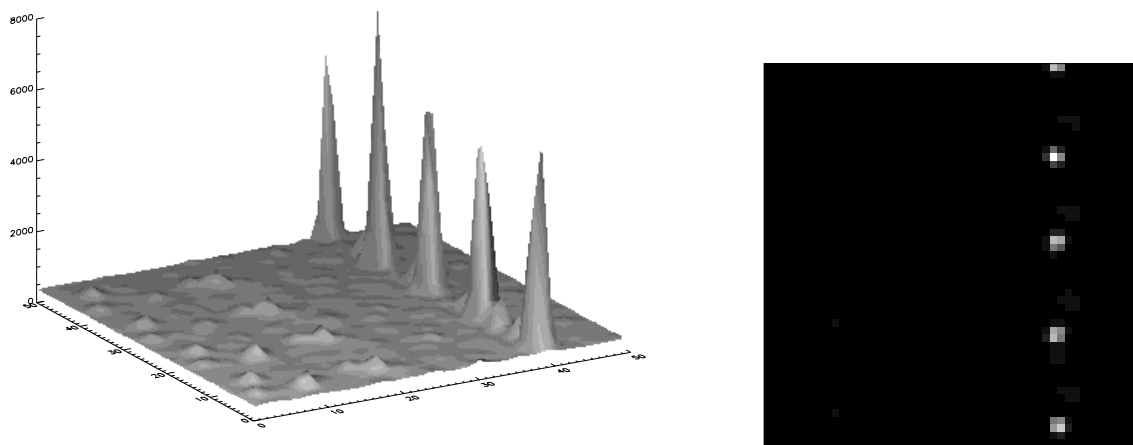

Figure 4: Surface plot and intensity plot of a section of simulated zipper mode image.

3 Noise and Signal

3.1 Noise

The images contain noise from several sources. There are random fluctuations in the photon counts, which are modeled as Poisson noise. Atmospheric turbulence causes photons originating from a particular source to fall onto different locations on the CCD detector at different points in time, giving rise to "image motion." The noise introduced by the CCD electronics (readout and dark noise) is assumed to follow a known Gaussian distribution. Additionally there may be stellar occultations by terrestrial (e.g. birds) and extra-terrestrial objects (e.g. asteroids), other than KBO's. Gamma ray bursts may inject photons; diminution and augmentation of star intensity may be due to the star being variable and not all variable stars are cataloged.

3.2 Signal

The occultation of a star by a KBO will result in a reduced photon count from the star for the *duration* of the occultation, where the *amplitude* of the occultation is a measure of this reduction. The *onset time* is defined as the time of arrival of the "signal," which is the reduction in counts from that star.

The signal is affected by the diameter of the KBO and the *impact parameter* of the occultation, which we define as the minimum angular distance over the KBO's trajectory between the center of the occulting KBO and the center of the star that is being occulted. If the impact parameter is zero, the path of the center of the KBO will cross that of the center of the star, so that for certain angular sizes of star and KBO, the reduction in counts from the star will be total, for at least one instance in time—see Figure 5.
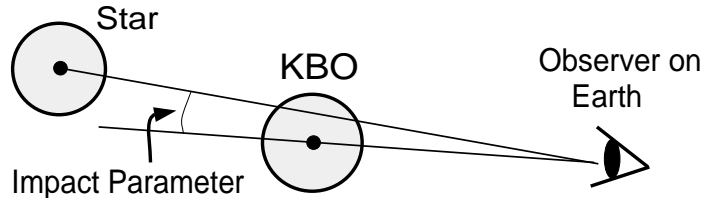

Figure 5: The impact parameter for the occultation of a star by a KBO.

We idealize a geometric occultation (one for which the effects of Fresnel diffraction are negligible) as a square wave for which the time of onset, amplitude (fractional decrease in flux), and duration are random. We do not think that phenomena ignored by this idealization significantly affect the results we report, since the test for an occultation will be based on total flux reduction during a hold and since shallow, brief occultations will have small detection probability. For fixed heliocentric distance and angle of observation, the joint probability distribution of the amplitude and duration is determined by the impact parameter and the diameter of the KBO. We assume that the impact parameter is uniformly distributed and that the KBO diameter follows a power law with parameter $\omega = 3.5$ equal to that for asteroids in the asteroid belt. Let $N(c)dc$ denote the number of KBO's with diameter between c and $c+dc$. We have, for c between c_{min} and c_{max}, the following approximation:

$$N(c)dc = N_0 \left(\frac{c}{c_0} \right)^{-\omega} dc \tag{2}$$

For observations near opposition, Figure 6 shows the resulting joint probability distribution of amplitude and duration, determined from the probability distributions of amplitude and duration. From the figures we see that the amplitude is typically about 0.3 and the duration is typically about 100ms.

Such probability models can be developed for a set of fixed heliocentric distances and fixed angles of observation. In the example above the angular size of all stars was fixed to be that of a four kilometer object at 50AU. We assume that the velocity of an object at each heliocentric distance is constant and equivalent to that for an object making a circular orbit.
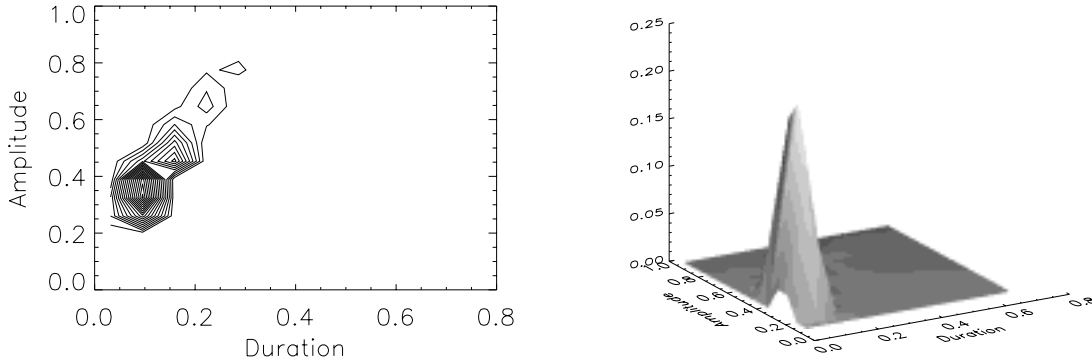
Figure 6: The joint probability density function of amplitude and duration (in seconds) when observing near opposition. The relative impact parameter is restricted to the interval [0,.9].

4   Detection Scheme

We wish to design statistically and computationally efficient detection algorithms, guided by theoretical arguments and simulations, keeping in mind that the algorithms should run in real time on a large number of star trails. The occultations are expected to be infrequent and for credibility the false alarm rate should be controlled at a small level, such as 10^{-12}. Since we expect to make 10^{10} to 10^{12} tests per year, this choice would lead to a false alarm rate of less than one per year.

Consider the measurement of the flux from a given star in one hold. In principle, using the idealizations above, the probability of that measurement can be evaluated under the assumption of no occultation and under the assumption that an occultation has occurred. This allows construction of a likelihood ratio test ([Rice, 1995]) which would be optimal if the idealizations and assumptions held. For computational considerations we use a simple approximation to this test. For further discussion of a likelihood ratio test and tests based on multiple holds see [Liang, 2001].

Consider first a single telescope. For a set of preliminary observations of each monitored star hold, we compute the median and the interquartile range of the sequence of flux measurements. These flux measurements could be obtained from summing up the counts in a pixel neighborhood (aperture photometry) or by fitting the point spread function (psf). (We are currently working on how to best extract flux measurements for individual stars from the CCD array in real time with the complications of overlapping and image motion.) These initial values are used to standardize subsequent flux measurements from that star: the median value is subtracted from the flux and the result is divided by the interquartile range. We use the median and interquartile range rather than

the arithmetic mean and standard deviation in order to guard against occultations and aberrant outliers. Let Y_{ksh} denote the resulting test statistic for hold h of star s on telescope k.

We now describe a test based on measurements at multiple telescopes which flags a star-hold if Y_{ksh} is sufficiently small at each telescope, based on the set of preliminary observations. Suppose the desired false alarm rate is α and there are K telescopes. For each telescope we pool all the standardized Y_{ksh} from the set of preliminary observations together to form an ordered set $X_{k1} \leq X_{k2} \leq \cdots \leq X_{kn}$ where n is the total number of star-holds. Let m_k be the integer such that $m_k/(n+1)$ is closest to $\alpha^{1/K}$. A new observation is now tested by standardizing its measurement at each telescope as above, yielding values $Y_{1sh}, \ldots, Y_{Ksh}$ and is flagged as an occultation if $Y_{ksh} \leq X_{km}$ at all telescopes. In words, a suitably small observation is found at each telescope based on the initial set and new observations are then flagged if they are smaller than each of these thresholds.

That this procedure has the desired false alarm rate α is due to the following fact: Let $Z_1, \ldots, Z_n$ be independent random variables from the same continuous probability distribution and denote the ordered observations as $Z_{(1)} < Z_{(2)} < \cdots < Z_{(n)}$. Let Z be another independent random variable having the same distribution. Then $P(Z < Z_{(m)}) = m/(n+1)$. The applicability of this result in our situation depends on some idealizations. First, we assume that the noise is independent between telescopes, which seems plausible if they are sufficiently far apart. This assumption is probably the most crucial and will have to be investigated once the telescopes are operational. Second we assume that the noise affecting the measurement in each star-hold is independent of that affecting others. This is reasonable for the noise arising from photon fluctuations and CCD electronics; it is less so for atmospheric turbulence, but that is at least local in time and space. Third we assume that when there is no occultation the probability distribution of Y_{ksh} does not depend on s or h. One of the purposes of the standardization described above is to make this latter assumption more valid: dividing by the interquartile range attempts to compensate for difference in variability among stars of differing magnitudes. All Y_{ksh} should then have approximately equal first and second moments. If the flux distributions were Gaussian, for example, the distributions of the standardized statistics would all be identical.

The time dedicated to collecting the preliminary set of observations used for calibrating the test as above need not be great. For example, suppose that 2000 stars are monitored with a hold time of 200ms on three telescopes Then in 100 seconds we can collect 10^6 star-holds on each telescope, and to set a false alarm probability $\alpha = 10^{-12}$, the procedure requires a minimum of 10^4 observations on each telescope

It is strictly appropriate to use this data-determined threshold only if there is no occultation during the preliminary collection stage, which would almost certainly be the case because of the rarity of occultations. However, even if there were one, the values of the ordered observations used to form the test would only be slightly perturbed.

There are significant advantages in this data-based method of setting a threshold. The alternative would be to rely on simulations, which might not be sufficiently realistic and would furthermore have to be tailored to each star field, sky level, and "seeing" (the extent to which images are blurred by light diffraction in the turbulent atmosphere).

As we state above, the strict validity of this method of determining a threshold assumes that the statistics Y_{ksh} have the same distribution, for fixed k. In reality this will probably not be exactly the case, in particular because of the effects of crowding. Although our standardization takes account of differing level and variability of the flux distributions of different stars, those distributions might differ in their shapes in other ways as well, for example, they might differ in skewness. Thus it is beneficial to eliminate some stars from the list of those monitored. The criterion we have been using is to identify in our simulations those stars that result in a large number of false alarms.

These false alarms are typically caused by a combination of image motion and nearby bright stars. Eliminating such stars in fact increases the chances of detecting occultations of others since their inclusion results in a more stringent threshold.

In principle we need not combine observations from different stars but could construct a different threshold for each star by applying the procedure described above star by star, with no pooling. If there were three telescopes, we would need about 30 minutes to collect 10^4 observations on each telescope, which would be just sufficient to construct a test with a false alarm probability of 10^{-12}. If there were four telescopes only 3 minutes would be required. An intermediate alternative would be to group the stars into homogeneous sets.

5   Selected Results from Simulations

We constructed a simulator incorporating zipper mode operation and the noise sources mentioned in Section 3.1 and occultations generated from the model described in Section 3.2. Simulated images may be used to determine operational parameters to maximize the detection rate.

The simulator takes a star field as input; in the results described below we used the USNO catalogue. We consider two star fields (1), which we will denote as Crowded Field (RA 4.905h, Dec 29.275degree) and Sparse Field (RA 9.61833h, Dec 0.7250degree). The Crowded Field has 56,044 stars and the Sparse Field has 11,467 stars in three square degrees. The catalogue is complete down to magnitude 17-18 and the sky background brightness was set equivalent to that of a star of of magnitude 20 (magnitude is a measure of the brightness of stars on a logarithmic scale with larger magnitudes corresponding to dimmer objects).

We first illustrate the advantages of using multiple telescopes revealed by a simulation, in which the telescopes were taken to be identical and independent. Table 1 shows the detection probability for different false alarm probability and differing numbers of telescopes, based on a simulation of 418 holds for each of 371 stars with around 1500 occultations generated from the distribution shown in Figure 6. From this table we see that using two telescopes rather than one enables us to reduce the false alarm rate from 10^{-4} to 10^{-8} with only a very slight decrease in detection rate. Introducing a third telescope has the effect of reducing the false alarm probability to 10^{-12}, while only decreasing the detection probability from 3.6% to 3.5%. If the false alarm probability is held fixed, the detection rate increases when more telescopes are used. Of course the details of these results depend upon the simulation and even more importantly upon operational parameters such as choice of star field and the background level of light in the sky. Qualitatively, the important conclusion is that by using more telescopes, false alarm probabilities can be drastically decreased with little loss in detection rates and that detection probabilities can be increased while the false alarm probability is held fixed. Although the detection probabilities are small, we note that there are many more dim stars than bright ones, and occultations of the former are much harder to detect. If only bright stars were monitored, the probabilities would be substantially larger (90% or more for magnitudes less than 10.5 or so), but there would be a loss in the total number of detections. This issue is discussed further below.

Decisions must be made about whether to observe near quadrature or opposition. On the one hand occultations observed at quadrature will have longer durations and thus should be easier to detect, but on the other hand there will be more occultations at opposition because the speed of a KBO relative to earth will be larger. Simulations can be used to investigate this tradeoff and Figure 7 shows a comparison. The value μ on the vertical axis is proportional to the expected number of occultations detected, assuming that the occultation rate is proportional to the relative speed of the KBO to earth. (The constant of proportionality depends upon the density of KBO's,

Table 1: False Alarm and Detection Probabilities for Single and Multiple Telescopes near Opposition. Stars with magnitude less than or equal to 15 were monitored.

One Telescope		Two Telescopes		Three Telescopes		Four Telescopes	
F.A. Prob	Detection Prob	F.A. Prob	Detection Prob	F.A. Prob	Detection Prob	F.A. Prob	Detection Prob
10^{-2}	0.187	10^{-4}	0.126	10^{-6}	0.110	10^{-8}	0.101
10^{-3}	0.095	10^{-6}	0.076	10^{-9}	0.060	10^{-12}	0.056
10^{-4}	0.036	10^{-8}	0.036	10^{-12}	0.035	10^{-16}	0.033

the number of stars monitored, and other factors as well). μ depends upon the cutoff magnitude for monitored stars as shown on the horizontal axis. From the figure we conclude that it is favorable to observe near opposition and that there is little gain in monitoring stars with magnitudes greater than 13.5. We note however, that near quadrature it is likely successive holds would be occulted, and a test that took into account multiple holds would result in higher detection rates. In one simulation this increase was of the order of 20%, which leads us to conclude that overall it is still favorable to observe near opposition.
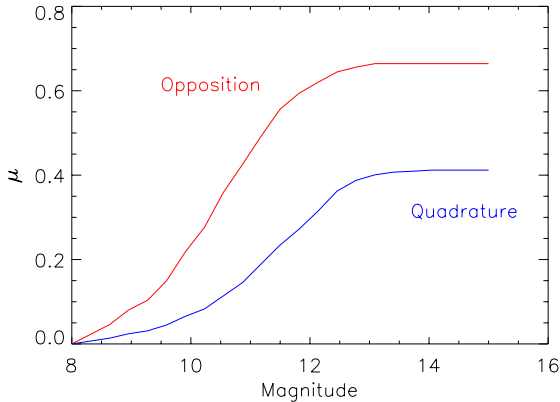

Figure 7: Comparison of the efficacy, μ, of observing near quadrature or opposition for the Crowded Field and a hold time of 200ms. Results are shown as a function of cut-off magnitude (i.e., only stars brighter than the cut-off magnitude are monitored).
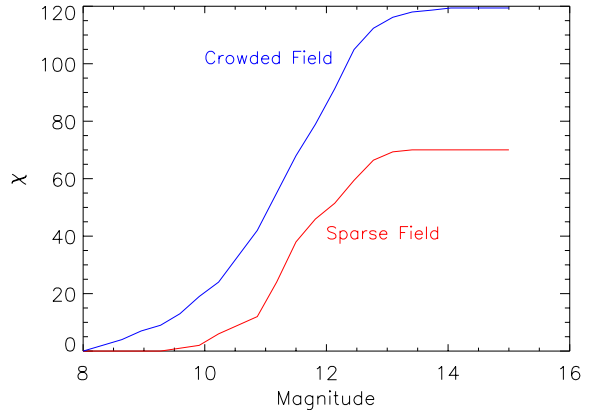

Figure 8: Comparison of the efficacy of observing near quadrature for the Crowded and Sparse Fields and a hold time of 200ms. The value χ is proportional to the expected number of occultations detected and is shown as a function of cutoff magnitude.

The choice of star fields to be monitored can also be guided by simulation. Again there are tradeoffs: although crowding may increase the noise level, especially when coupled with image motion, making the detection of individual occultations more difficult, a larger number of stars would be monitored hence increasing the number of occultations per unit time. Figure 8 compares the expected number of occultations detected in a crowded versus a sparse field. We see that there are substantial gains to be made in monitoring the crowded field.

The simulator thus has great utility in guiding the choice of various operational parameters. As a further example, we can examine the effects of alternative choices of zipping parameters the duration of holds and the number of shifts between holds) for different angles of observation and different phases of the moon.

6 Retrospective Estimation of Occultation Rate

In the previous section we focused on detecting occultations in real or near-real time. This would enable discovery of particular objects, some of which might be large enough to follow up optically. Beyond this however, there is great interest in estimating the total abundance of KBO's or at least placing bounds on this quantity, since essentially nothing is known about the small (km sized) population. Such information will help constrain theories of the formation of our solar system. Thus we would wish to try to pool the results of observations over a long period of time, such as a year, to address this question. Note that there is a distinction between making and enumerating detections in real time as compared to such retrospective studies. For example, in a retrospective mode, one is not as interested in which particular events showed occultations as in estimating the total number of such events. Thus, different methods of statistical analysis may be appropriate in the two endeavors.
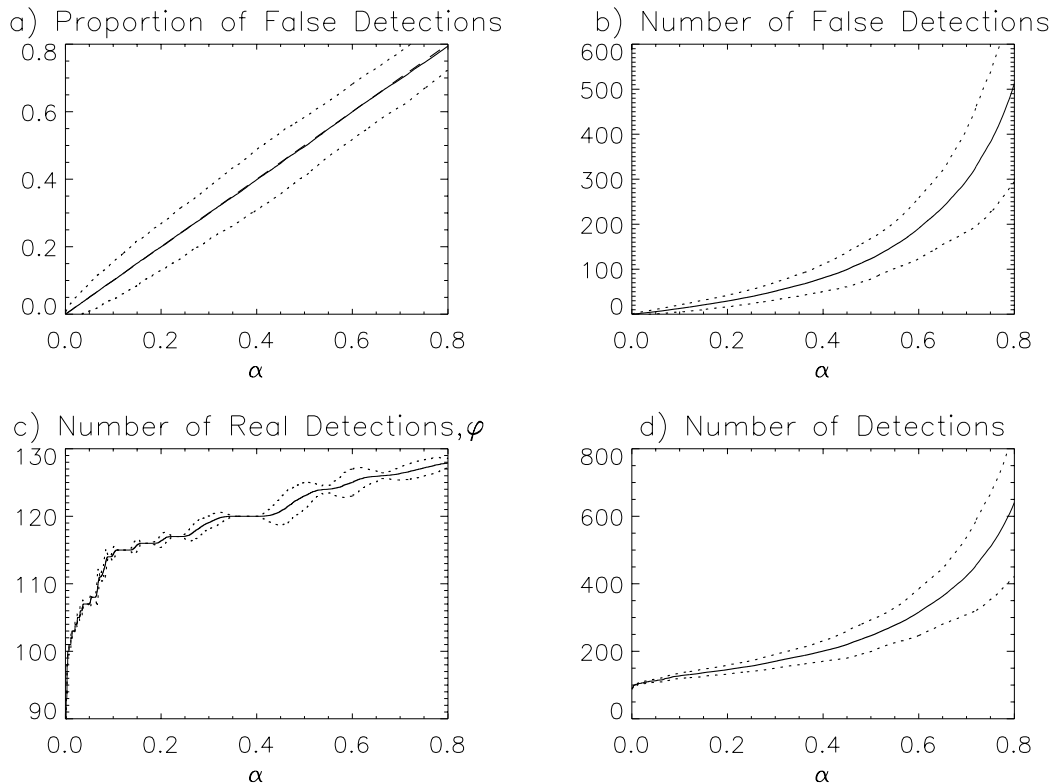

Figure 9: Mean (Unbroken) $\pm$ 2 standard deviations (Dotted), using 200 repetitions, for a) Proportion of False Detections; b) Number of False Detections; c) Number of Real Detections, φ_α; d) Number of Detections. $n = 10^{10}$ and number of occultations = 300.

From a year of observing, we would have archived the p-values of $10^{10} - 10^{12}$ tests. In all but

a tiny fraction of cases, the null hypotheses will have been true. This unknown fraction λ, the occultation rate, could be as large as 10^{-7}, but is unknown even to an order of magnitude. The distribution of P-values under the null (no occultation) is uniform. The distribution of the P-values under the alternative is not identical from test to test, but depends on the star being monitored and other operational parameters that are not constant. Were the marginal distribution of P-values under the alternative known, or if it could be reliably estimated by simulation, one could consider fitting a mixture to the empirical distribution of all the P-values, but this is not the case. In some simulations, we found the estimate of λ not robust to mis-specification of the distribution of P-values when there is an occultation.

The most promising approach to retrospective analysis that we have found is based on the concept of the "False Discovery Rate." The aim of the testing method described earlier is to control the expected number of false alarms per unit time by controlling the false alarm probability to be at a desired value γ. The aim of a recently proposed procedure [Benjamini and Hochberg, 1995] is different; it proposes to control the expected proportion of flagged signals which are false alarms— the False Discovery Rate (FDR). The procedure works as follows. Suppose that n independent hypotheses have been tested with corresponding ordered p-values, $p(1) \leq p(2) \leq \cdots \leq p(n)$. In our case these would be p-values determined as described above in section 4 for all the n occultation tests conducted during the period under consideration. Let $0 < \alpha < 1$ be the desired value for the FDR and let k be the largest integer such that $p(k) \leq \alpha k/n$. Then if hypotheses corresponding to $p(1), \ldots, p(k)$ are rejected, the FDR is less than or equal to α. To contrast the two approaches, note that an event is flagged by the former procedure if it's p-value is less than γ, whereas it is flagged by the FDR procedure depending on the rank of its p-value, which could only be determined retrospectively.

This procedure is illustrated in the following simulation. Suppose we monitor stars of magnitude less than or equal to 13.5 (see Figure 7) using three telescopes. For $n = 10^{10}$ and 300 real occultations, generated from the model described in Section 3, the FDR procedure was implemented for α ranging from 0 to 0.8. Figure 9 shows the results of replicating this 200 times. Figure 9(a) is especially noteworthy. We see that FDR is very close to α, not merely less than or equal to α over the entire range of α. Also, the variance is small. For comparison, if the procedure controlling the false alarm probability to be 10^{-12} was used, the detection probability in this simulation would have been 21.8% and thus we would expect 65 occultations to be detected. (The detection probability is substantially higher than in Table 1 because of the magnitude cut-off.) By contrast, if FDR were used to determine a subset with α equal to .05 or .10, we see from Figure 9(c), that more than 100 real occultations would be included.

Figure 9(a) suggests that if FDR is controlled at level α, the proportion of false detections will in fact be quite close to α. Thus if the number of flagged signals is Ω_α, it is natural to estimate the number of real detections among them by $\hat{\varphi}_\alpha = (1 - \alpha) \times \Omega_\alpha$. Figure 10 shows the error in estimating φ_α as a function of α. We see there that the error is small, but increases as α increases.

As noted above, the fraction of star-holds in which occultations occurred would provide important information about KBO abundance. We thus propose a method for estimating the occultation rate.

We note that the number of occultations will be greater than or equal to the number of real detections. An estimated lower bound for the number of occultations will then be given by $\hat{\varphi}_\alpha$. We define λ to be the occultation rate in our data, given by the ratio of the number of occultations to the total number of tests conducted. In this way, lower bounds for λ as a function of α are estimated by $\hat{\lambda}_\alpha = \hat{\varphi}_\alpha/n$. The number of real detections will increase with α so, viewing $\hat{\lambda}_\alpha$ as an estimate of λ, the bias will decrease as α increases. On the other hand, the variance increases with
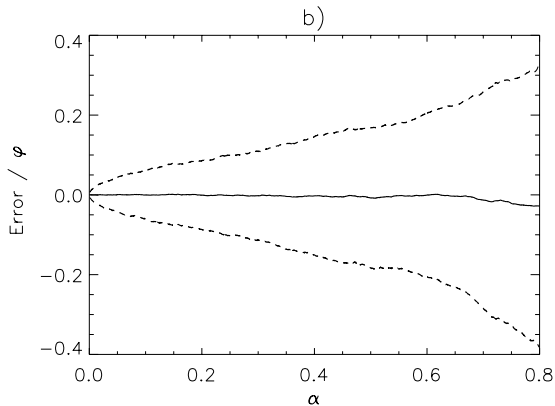
Figure 10: The Proportional Error (mean plus or minus 2 SD's) in Estimates of φ_α in 200 Repetitions. $n = 10^{10}$ and number of occultations = 300.
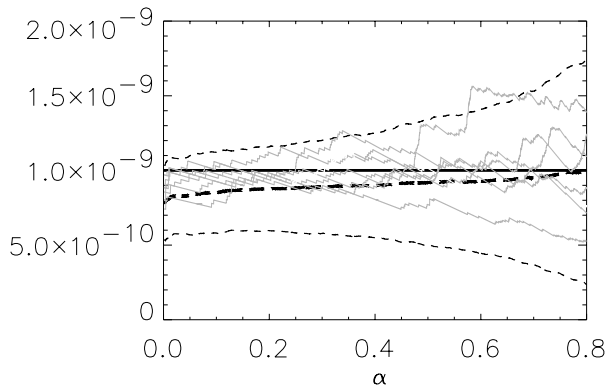
Figure 11: The average value (bold dash) plus and minus two SD's (faint dash) for $\hat{\lambda}_\alpha$ versus α, when $\lambda = 10^{-9}$(bold unbroken) , together with $\hat{\lambda}_\alpha$ in 6 simulations (light grey lines). Number of Tests $= 10^{11}$. A cutoff magnitude of 11 was used.

increasing α as shown in Figure 10. Both these effects are shown in Figure 11.

As noted previously, the brighter the star, the higher the detection probability in general, so it may be beneficial to limit estimates to brighter stars for the purpose of estimating the occultation rate. In Figure 12 we see that as λ increases, the relative error decreases. When only relatively bright stars are used, it appears that smaller values of α result in superior performance. However, if fainter stars are used as well, the optimal value of α seems to depend on the number of tests and the value of λ. Overall, it is encouraging that the RMS error is not terribly sensitive to the value of α.
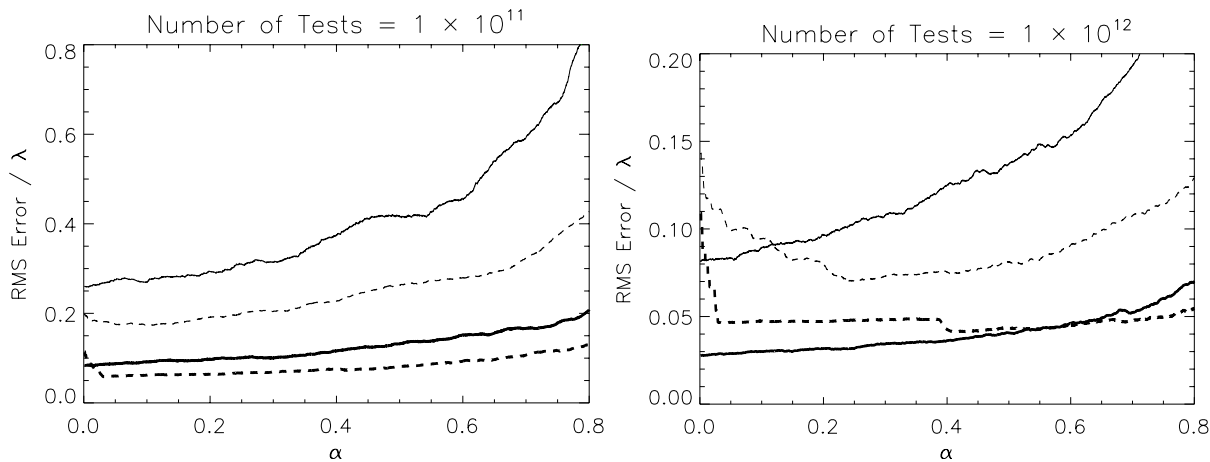

Figure 12: Relative RMS error in estimating λ. Number of Tests, near quadrature: (left) 1×10^{11}, (right) 1×10^{12}. Bold: $\lambda = 5 \times 10^{-9}$, faint: $\lambda = 5 \times 10^{-10}$. Cut-off magnitude: (unbroken) 11.0, (dashed) 12.1.

7   Conclusion

We have shown how multiple telescopes may be used to control the false alarm rate for real-time detection, by using thresholds determined in a data-based manner. Realistic simulations illustrated the effectiveness of this procedure and may be used to guide the choice of various operational parameters. We have argued that once a substantial body of data has been gathered, an alternative method based on the FDR procedure can be used to estimate the occultation rate. Simulations indicate that this method can produce useful results. It is important to note that different statistical procedures are appropriate for real time detection as compared to retrospective analysis.

The data archive resulting from TAOS will be a valuable resource for other astronomical research as well. For example, little is known about stellar variability on a sub-second level and TAOS will provide a vast collection of such time series. There may well be unexpected phenomena in the archive and in order not to miss them we face a problem of searching for needles in a haystack when we don't know what needles look like. How can we automate serendipity?

References

[Axelrod et al., 1992] Axelrod, T., Alcock, C., Cook, K., and Park, H. (1992). A direct census of the Oort cloud with a robotic telescope. *ASP Conf. Ser. 34: Robotic Telescopes in the 1990s*, pages 171–181.

[Bailey, 1976] Bailey, M. (1976). Can invisible bodies be observed in the solar system. *Nature*, 259:290–291.

[Benjamini and Hochberg, 1995] Benjamini, Y. and Hochberg, Y. (1995). Controlling the false discovery rate: a practical and powerful approach to multiple testing. *J. R. Statist. Soc*, 57:289–300.

[Edgeworth, 1949] Edgeworth, K. (1949). The origin and evolution of the solar system. *Mon. Not. Roy. Astr. Soc.*, 109:600–609.

[Fernandez, 1980] Fernandez, J. (1980). On the existence of a comet belt beyond Neptune. *Mon. Not. Roy. Astr. Soc.*, 192:481–491.

[Jewitt, 1999] Jewitt, D. (1999). Kuiper belt objects. *Annual Review of Earth and Planetary Sciences*, 27:287–312.

[Jewitt and Luu, 1993] Jewitt, D. and Luu, J. (1993). Discovery of the candidate Kuiper belt object 1992 qb1. *Nature*, 362:730–732.

[Kuiper, 1951] Kuiper, G. (1951). *In Astrophysics: A Topical Symposium*, pages 357–424.

[Liang, 2001] Liang, C.-L. (2001). *The Detection of Stellar Occultations by Kuiper Belt Objects*. PhD thesis, Department of Statisitcs, University of California, Berkeley.

[Rice, 1995] Rice, J. (1995). *Mathematical Statistics and Data Analysis*. Duxbury Press.

[Stern, 1996] Stern, S. A. (1996). The historical development and status of Kuiper disk studies. *PASP*, 107.

[Weissman, 1995] Weissman, P. (1995). The Kuiper belt. *ARAA*, 33:327–358.